감성과학
제21권 3호, 2018
<연구논문>

pISSN 1226-8593
eISSN 2383-613X
Sci. Emot. Sensib.,
Vol.21, No.3, pp.83-102, 2018
https://doi.org/10.14695/KJSOS.2018.21.3.83

Differences in Large-scale and Sliding-window-based Functional Networks of Reappraisal and Suppression

Suhnyoung Jun* · Seung-Koo Lee** · Sanghoon Han*,***†

*Department of Psychology, Yonsei University

**Department of Radiology, College of Medicine, Yonsei University

***Graduate Programs in Cognitive Science, Yonsei University

Abstract

The process model of emotion regulation suggests that cognitive reappraisal and expressive suppression engage at different time points in the regulation process. Although multiple brain regions and networks have been identified for each strategy, no articles have explored changes in network characteristics or network connectivity over time. The present study examined (a) the whole-brain network and six other resting-state networks, (b) their modularity and global efficiency, which is an index of the efficiency of information exchange across the network, (c) the degree and betweenness centrality for 160 brain regions to identify the hub nodes with the most control over the entire network, and (d) the intra-network and inter-network functional connectivity (FC). Such investigations were performed using a traditional large-scale FC analysis and a relatively recent sliding window correlation analysis. The results showed that the right inferior orbitofrontal cortex was the hub region of the whole-brain network for both strategies. The present findings of temporally altering functional activity of the networks revealed that the default mode network (DMN) activated at the early stage of reappraisal, followed by the task-positive networks (cingulo-opercular network and fronto-parietal network), emotion-processing networks (the cerebellar network and DMN), and sensorimotor network (SMN) that activated at the early stage of suppression, followed by the greater recruitment of task-positive networks and their functional connection with the emotional response-related networks (SMN and occipital network). This is the first study that provides neuroimaging evidence supporting the process model of emotion regulation by revealing the temporally varying network efficiency and intra- and inter-network functional connections of reappraisal and suppression.

Key words: Emotion Regulation, Reappraisal, Suppression, Dynamic Functional Connectivity, Graph Theory

---

※ This work was partially supported by the Yonsei University Future-leading Research Initiative of 2017(#2017-22-0136) and Basic Science Research Program through the National Research Foundation of Korea (NRF) funded by the Ministry of Science, ICT & Future Planning (#2015-R1A2A2A04006136).

† Corresponding Author : Sanghoon Han (Department of Psychology, Graduate Programs in Cognitive Science, Yonsei University)
E-mail : sanghoon.han@yonsei.ac.kr
TEL : 02-2123-5436
FAX : 02-2123-8330

1. Introduction

Humans have developed several emotion regulation strategies that help them maintain composure by avoiding and alleviating negative emotional experiences (Gross, 2002). Two regulatory strategies, cognitive reappraisal and expressive suppression, have been studied widely and are the most commonly adopted strategies (Gross & John, 1998). According to the process model of emotion regulation (Gross, 2002; Gross & John, 1998, 2003; Sheppes & Gross, 2011), reappraisal and suppression are antecedent-focused top-down regulatory and response-focused strategies, respectively. Reappraisal occurs in the early emotion-generative process and suppression in the final stage thereof. Reappraisal involves detecting and encoding incoming emotional stimuli and controlling the interpretation of the stimuli cognitively while suppression involves restraining affective behavioral responses against the stimuli (Gross & John, 2003). Literature has shown the differences between reappraisal and suppression in brain engagements and functional connectivity (FC) and the superiority of reappraisal (Cutuli, 2014; Gross & John, 2003; Hayes et al., 2010; Ochsner & Gross, 2008; Ochsner et al., 2004). However, neuroimaging studies have failed to provide specific and direct evidence to support the temporal distinction between reappraisal and suppression because most functional MRI studies have adopted the temporal stationarity assumption and performed a simple seed-based FC analysis.

Traditional stationary FC analysis, combined with graph theory (Bullmore & Sporns, 2009; Rubinov & Sporns, 2010; van den Heuvel & Hulshoff Pol, 2010), enables quantitating topological characteristics of functional brain networks. Various studies have made remarkable developments in understanding the large-scale properties of brain function (Hutchison, Womelsdorf, Allen, et al., 2013). Recently, research has focused on the temporally varying nature of the BOLD signal and demonstrated the temporal variations of the resting-state networks across a single scan (Allen et al., 2014; Chang & Glover, 2010; Di & Biswal, 2015).

A sliding-window correlation (SWC) analysis has been widely employed to investigate *dynamic functional connectivity*. It has ensured its use in various task fMRI experiments examining visual, learning, recollective memory, and executive function (Bassett et al., 2011; Braun et al., 2015; Cole et al., 2013; Di et al., 2015; Fornito, Harrison, Zalesky, & Simons, 2012) and has shown its potential in revealing that spatiotemporally static FC patterns are comprised of multiple discrete states (Allen et al., 2014; Hutchison, Womelsdorf, Allen, et al., 2013; Kiviniemi et al., 2011). However, there is a paucity of studies regarding task-related temporal dynamics, and, as a result, the time-varying pattern of the functional recruitment of brain regions during the performance of reappraisal and suppression remains unclear.

The primary purpose of this study was to provide the first direct empirical neuroimaging evidence of the time difference between the reappraisal and suppression suggested by the process model of emotion regulation by employing graph theory and the SWC analysis. Furthermore, we investigated the properties of functional brain networks at various levels and compared the behavioral performance of the two strategies to uncover the differences in network properties between the reappraisal and suppression.

2. Methods

2.1. Participants

Thirty participants (13 females) were recruited for monetary compensation from a college research recruitment database. They were screened for any significant medical conditions including a history of any psychiatric disorder, and none was excluded. Of the participants who had performed the task in the fMRI scanner, three parti-

cipants were excluded; two because of excessive movement and one because of incompletion of the fourth run and extreme fatigue. Thus, the sample comprised 27 participants (12 females) aged 21-33 (mean age ± standard deviation (SD): 25.41 ± 2.53 years; all right-handed). All participants provided written informed consent for procedures approved by the Institutional Review Board of Yonsei University (1040917-201312-HRBR-02-03).

2.2. Stimuli

Visual stimuli were selected from the EmoMadrid emotional pictures database (http://www.uam.es/gruposinv/ceaco/EmoMadrid.htm). Before the experiment, we recruited 17 subjects for a pilot test to have them give a valence assessment on a scale of 1 ("feeling neutral") to 5 ("strongly unpleasant and disturbing") about the 128 images (85 negative images and 43 neutral images) provided by the EmoMadrid. Among the neutral images, 16 images with the average valence rating most close to 1 (mean ± SD = 1.19 ± .09) were used for the main experiment. After excluding top 5% (that is, 4 images) of the negative images whose average valence score were closest to 5 in order to prevent the possible risk of participants experiencing too negative emotions, forty-eight negative images (mean ± SD = 3.14 ± .45) were used for the main experiment.

A day before engaging in the fMRI task, the demographic and mood- and anxiety-related self-report questionnaires were collected to exclude potential psychiatric disturbances: the Beck Depression Inventory , the Dysfunctional Attitude Scale , and the Beck Anxiety Inventory (Beck & Steer, 1988). Also, all participants rated the valence of 128 images on a scale of 1 ("feeling neutral") to 5 ("strongly unpleasant and disturbing"). For each of the three conditions (reappraisal, suppression, and habitual regulation) 16 negative images were randomly allocated, and the pre-rated valence of the negative images was equated across the conditions [$F(2, 45) = .31$, $p > .73$]. Then, each condition has either 16 negative images or 16 neutral images in total. Again, as the same images were used for run1 and run3, and for run2 and 4, the 16 images of each condition were randomly distributed to two sets; each set with 8 images. As a consequence, each run consisted of 24 negative images and 8 neutral images, and the order of images was randomized.

The followings are the mean valence ratings of the images used in the experiment ± SD: reappraisal = 3.16 ± .44; suppression = 3.15 ± .51; habitual = 3.04 ± .42; and passive view = 1.27 ± .10. Compared to the neutral images in the passive view condition, the negative images in cognitive reappraisal [$t(15) = 15.96$, $p < .0001$], the negative images used in expressive suppression [$t(15) = 14.29$, $p < .0001$], and the negative images used in habitual regulation [$t(15) = 17.16$, $p < .0001$] had a statistically significant lower valences.

2.3. Procedure

The *Emotion Regulation Task* for the fMRI acquisition consisted of four runs. Stimuli were presented in a blocked design and the blocks in a fixed order; each block comprised eight trials (duration per trial: 24 s) taken from one of the four regulation conditions. A resting phase (24 s) occurred after the first two blocks. Each trial involved a fixation cross in the center of the screen (2 s); a cue, assigning the emotion regulation strategy to be used (4 s); another fixation cross (2 s); an emotion regulation phase when participants watched an emotion-eliciting image (neutral for passive view condition) and practiced the cued strategy (12 s); and a response phase (4 s) when participants expressed their feelings at that moment on a scale of 1 ("feeling neutral") to 5 ("strongly unpleasant and disturbing")(Fig. 1). As a result, the total length of a run was 13 min 12 sec including the resting phase of 24 sec put between the block 2 and block 3.

The block and images were fixed-ordered, rather than

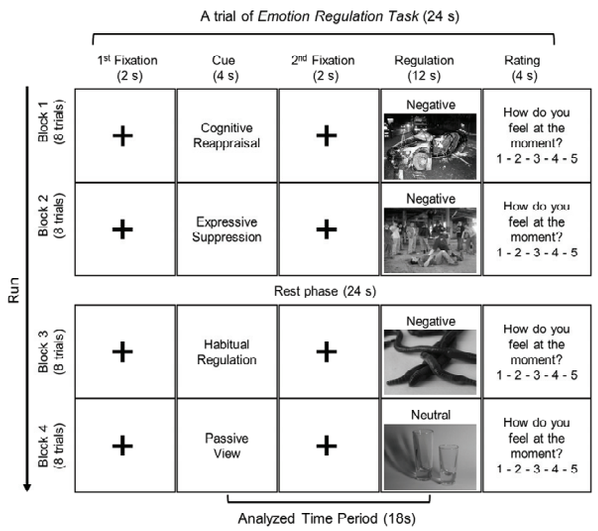

Fig. 1. Procedures of an experimental run, which was repeated four times. The order of the blocks and the images were fixed to ensure the uniformity of the temporal dynamics of participants' functional brain time series across participants

randomized, to ensure uniformity in the temporal dynamics of participants' functional brain time series across participants. Possible confounding effects of the fixed order were acknowledged. The design was insisted, however, for following reasons: to (1) counterbalance or minimize the effects of the images' characteristics on brain activity as participants used the same emotion regulation strategy for the same images in the same order; (2) engender generalized brain activity during the block by averaging the voxel-wise time series for all participants and the use thereof to speculate the dominant temporal flow of time series during the performance of the strategies; (3) compare the yielded time series between the conditions and identify the distinctive dynamic features for each condition; and (4) match the generalized dynamic features observed from the empirical brain imaging data with theoretically suggested procedures of emotion regulation.

The participants were trained for the fMRI task. For the reappraisal trials, they had to acknowledge their emotion and think positively about the stimuli. For the suppression trials, they were to become detached from the scene, or emotion elicited thereof and not make facial expressions. For the habitual-regulation trials, participants were to calmly employ a strategy that was not confined to reappraisal or suppression. For the passive view trials, they were to look at the image and express emotions naturally. They were allowed a 5-minute practice on a laptop to rehearse each strategy. While practicing, participants were required to orally present how they understand the strategy, and which thought process they are using to accomplish the strategy so that the experimenter can help them use right strategy and review their performance. Depending on their understanding of the strategy and proficiency of performance, the length of practice run varied (~up to 20 minutes). All participants were able to start the experiment only after the experimenter was ensured of their full understanding of the strategies.

The experimental task and recording of the presentation time of the images and behavioral responses were conducted by utilizing Matlab R2016b (The MathWorks, Inc., Natick, MA) and Cogent toolbox (www.vislab.ucl.ac.uk/Cogent). The participants viewed the experiment using the scanner through an MR-compatible mirror and responded using a five-button MR-compatible button pad.

2.4. fMRI data acquisition and preprocessing

We performed a functional MRI on a 3T GE MRI scanner (GE Healthcare, Waukesha, WI) using an 8-channel head coil. Functional images were obtained using an interleaved gradient echo-planar pulse image (EPI) sequence with the following parameters: repetition time (TR) = 2000 ms, echo time (TE) = 30 ms, voxel size = 3.75 × 3.75 × 4 mm, flip angle = tilted 30° from the AC-PC plane, field of view (FOV) = 220 × 220 mm, and number of axial slices = 33. For an anatomical reference, we acquired a high-resolution T1-weighted image using a 3D T1-turbo field echo (TFE) sequence (TR = 8.0 ms, TE = 3.7 ms, voxel size = 1 × 1.08 × 1 mm, and acquisition matrix = 240 × 222; number of slices = 216). Vacuum molded cushions and soft pads supported the subjects' head and minimized head movement.

Functional images were preprocessed using Statistical Parametric Mapping 12 (SPM12, http://www.fil.ion.ucl.ac.uk/spm/software/spm12/) under Matlab R2016b environment (http://www.mathworks.com). The first five functional images (10 s) were discarded to allow the MR signal to achieve equilibration. Preprocessing process included slice-timing correction, head-motion correction, co-registration to the subject's high-resolution anatomical images, segmentation to create a spatial normalization deformation field and bias-corrected structural image, normalization, regressing out head-motion parameters using the Friston 24 parameter model (Friston, Williams, Howard, Frackowiak, & Turner, 1996), and spatial smoothing using 8 mm full-width at half-maximum (FWHM). Recent work showed that regressing out Friston 24-parameters is more effective than other movement correction methods (Takeuchi et al., 2017; Yan et al., 2013).

To include the preparatory cognitive recruitment for emotion regulation and exclude neural activity for the valence rating step, three phases (i.e., cue, second fixation cross and the regulation of nine volumes; total 18 s) were selected among the five phases of the trial for the future analyses.

2.5. Behavioral Analysis

Task performance was defined as the degree of neutralization and was computed for each condition. The formula employed was:

$$\text{Degree of neutralization} = \frac{(Vpre - Vtask)}{Vpre} \times 100$$

Vpre is the mean of the pre-rated valence of the images of a given condition. *Vtask* is the average of the valence rated during the task. The degree of neutralization was obtained for each condition and subject. An independent *t*-test was conducted to compare the means between reappraisal and suppression conditions. All demographic and behavioral data were analyzed using Matlab. Probability values of $p < 0.05$ were accepted as statistically significant.

2.6. Large-scale network

For cortical parcellation, we used a collection of 160 regions of interest (ROIs) (Dosenbach et al., 2010) which were previously reported to construct six resting-state brain networks (RSNs): the cerebellum network (CN), cingulo-opercular network (CON), default mode network (DMN), frontoparietal network (FPN), occipital network (ON), and sensorimotor network (SMN)(Dosenbach et al., 2007; Dosenbach et al., 2006; Fair et al., 2009); See Fig. 2 for details. The smoothed time series of the blocks of the same condition from all runs were concatenated for each subject. For each brain region, the time series of voxels included were averaged, and the FC between any two ROIs (paired ROIs) was assessed with the Pearson's correlation analysis. For each subject, there were 12,720 (160 × 159 / 2) *r* values in the cross-correlation matrix, and the matrix was converted into *z* map by Fisher's *r-to-z* transformation. Then, we used *z* values as FC levels. Ergo, the “FC” refers to the z values

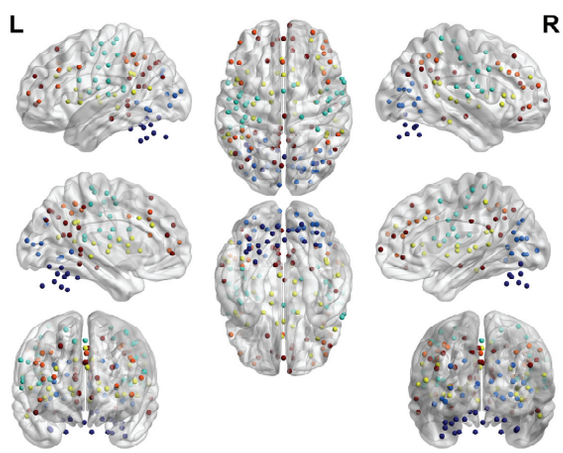

Fig. 2. Anatomical location of 160 regions-of-interest (ROIs). Regions are colored by network membership. Red, default mode network (DMN); orange, frontoparietal network (FPN); yellow, cingulo-opercular network (CON); light blue, sensorimotor network (SMN); blue, occipital network (ON); dark blue, cerebellar network (CN))

of each map.

To eliminate the meaningless and spurious functional connections which may obscure the topology of strong and significant connections in the functional network matrix, an absolute, or a proportional weight threshold is often applied (Rubinov & Sporns, 2010). As there is a large controversy over the method to determine the threshold (Hutchison, Womelsdorf, Allen, et al., 2013) and, thus, threshold values are often arbitrarily determined. In the present study, to carefully examine the effect of threshold, we explored several threshold levels (i.e., $|z| > 0.25$, 0.52, 0.84, 1.28, 1.65, and 1.96; each corresponding to the r value of > 0.25, 0.48, 0.69, 0.86, 0.93, and 0.96, respectively) (De Vico Fallani, Richiardi, Chavez, & Achard, 2014). In the paper, the results of the threshold of $r > .93$ are presented.

2.6.1. Computation of network metrics and key nodes

We examined the network characteristics of the FC matrix by calculating the two most robust measures of network topology: modularity (Q_{max}) and global efficiency (E_{glob}). Refer to (Rubinov & Sporns, 2010) for a review. We also computed two network metrics for every node in the network: the degree (*Deg*) and the betweenness centrality (*BC*). The degree of a node is a fundamental measure; it reveals the number of links connected to the node. The betweenness centrality is a measure of centrality in a graph based on shortest paths. For every pair of nodes in a weighted, connected graph, there exists at least one shortest path between the nodes which the sum of the weights of the edges is minimized. The betweenness centrality for each node is the number of these shortest paths that pass through the node. The Brain Connectivity Toolbox (BCT, http://www.brain-connectivity-toolbox.net) (Rubinov & Sporns, 2010) was used to compute the nodal measures. Thresholded, non-binarized, and undirected matrices were used.

For each individual, the two network metrics were calculated at the whole-brain network and the six RSNs of reappraisal and suppression. Paired *t*-tests were performed to examine the differences in the metrics between reappraisal and suppression. For each condition, we computed degree and betweenness centrality for each node and averaged across the subjects. Then, we selected the nodes with the highest degree and the highest betweenness centrality.

2.6.2. The intensity of inter- and intra-RSN FC

To examine the topological and functional relations among the six networks (i.e., CN, CON, DMN, FPN, ON and SMN) which were identified and organized by Dosenbach's research group (Dosenbach et al., 2007; Dosenbach et al., 2006; Fair et al., 2009), the mean strength of FC between every pairwise RSN connections (inter-RSN) and within each RSN (intra-RSN) were computed for reappraisal and suppression from each subject. Then, paired *t*-tests on the mean FC between reappraisal and suppression were performed.

2.7. Sliding-window correlation analysis

Although run effects could be traded in the general FC manner as in the case of the large-scale network analysis, they could engender mathematical problems when calculating the FC in a temporal window where two runs intersect. Thus, the runs were not concatenated in the SWC analysis. Previous studies showed that that the window length (l) should be shorter than the task block (Di et al., 2015), cognitive states could be identified with high accuracy with imaging runs as short as 30-60 s (Shirer, Ryali, Rykhlevskaia, Menon, & Greicius, 2012), the non-stationary nature of the brain's modular organization stabilized at a window size of roughly 33 s (Jones et al., 2012), and the results of the SWC analysis were similar across window lengths ranging from 30 to 240 s (Hutchison, Womelsdorf, Gati, Everling, & Menon, 2013). In the present study, to carefully examine the effect of the window length, we explored several window lengths (i.e., l = 18 TR, 27 TR, and 36 TR; each corresponding to 36 s, 54 s, and

72 s, respectively). Overlapping window size was determined to contain approximately 90% of the window length; thereby, 2 TR, 3 TR, and 4 TR for each window length. Furthermore, we explored the two thresholds: $r > .93$ and .98, each corresponding to the z score of 1.65 and 2.33. In the paper, the results of the window length of 18 TR resulting in a total 28 windows with the threshold of $r > .93$ are presented as we figured the window length (1.5 times longer than the trial length) would be short enough to reflect the dynamics across individual trials and long enough to capture the stable characteristics of the functional brain network at a window.

2.7.1. Computation of window matrix and network metrics

For every window of a subject, we computed a Fisher's r-to-z transformed cross-correlation matrix. Then the two network metrics were calculated at the whole-brain network and the six RSNs of reappraisal and suppression. Then, for each window, paired t-tests were performed to examine the differences in the metrics between reappraisal and suppression of intensity of inter- and intra-RSN FC.

2.7.2. Temporal changes of intensity of inter- and intra-RSN FC

We further computed the mean strength of FC between every pairwise RSN connections (inter-RSN) and within each RSN (intra-RSN) for each window of every subject. Then, paired t-tests on the mean FC between reappraisal and suppression were performed.

3. Results

3.1. Behavioral results

The paired t-test on the degree of neutralization analysis was conducted to investigate how much did the valence ratings on negative images change after performing a given emotion regulation strategy compared to pre-rated valence. Although the degree of neutralization of reappraisal ($M = 0.35$, $\sigma = 0.17$) and suppression ($M = 0.37$, $\sigma = 0.20$) was not statistically different ($t(26) = -0.43$, $p = 0.67$), the absolute value of valence ratings of reappraisal (M = 1.56, σ = 0.47) displayed a trend of lower valence rating than of suppression ($M = 1.78$, $\sigma = 0.80$) during the *Emotion Regulation* Task, $t(26) = -1.91$, $p = .07$).

3.2. Large-scale network analysis

3.2.1. Network metrics of the whole-brain network and the six RSNs

Network metrics analysis showed that the mean modularity of reappraisal ($Q_{max} = 0.51$) was significantly higher than that of suppression ($Q_{max} = 0.48$); thus, in general, the reappraisal network had dense connections between the nodes within modules and relatively sparse connections between nodes in different modules in the network than the suppression. There were no significant differences between the whole-brain network of reappraisal and suppression in the mean global efficiency. The CN revealed significantly higher modularity, and lower efficiency of information transfer across the network (i.e., global efficiency) during reappraisal than suppression. In addition, compared to suppression, the FPN and SMN also showed significantly higher modularity during reappraisal (Table 1).

3.2.2. Key nodes of the whole-brain network and the six RSNs

In the whole-brain network of both reappraisal and suppression, the left inferior frontal opercular (MNI coordinates = -55, 7, 23), a member of the SMN, had the highest degree, and the right inferior orbitofrontal cortex (MNI coordinates = 46, 39, -15), a member of the DMN, had the highest betweenness centrality (Table 2).

To see the brain region in each RSN that have the most controlling power over the whole-brain network,

Table 1. Differences in network metrics between reappraisal and suppression

	Q_{max}			E_{glob}		
	Reappraisal	Suppression	*t* value	Reappraisal	Suppression	*t* value
WBN	.51 ± .29	.48 ± .28	2.12*	.20 ± .29	.21 ± .29	-1.18
CN	.47 ± .24	.37 ± .28	2.27*	.26 ± .32	.29 ± .35	-2.16*
CON	.45 ± .26	.45 ± .27	.04	.19 ± .31	.19 ± .31	-.73
DMN	.49 ± .28	.52 ± .24	-.83	.15 ± .26	.15 ± .26	-1.30
FPN	.45 ± .27	.36 ± .28	2.86**	.17 ± .32	.18 ± .32	-.99
ON	.39 ± .27	.38 ± .27	.48	.19 ± .34	.19 ± .34	-1.00
SMN	.45 ± .25	.38 ± .25	3.36***	.24 ± .33	.24 ± .34	.12

Table 1 Paired *t*-tests were performed to examine the difference in network metrics between reappraisal and suppression. Values indicate mean ± standard deviation. Q_{max}, modularity; E_{glob}, global efficiency; WB, whole-brain network; CN, cerebellum network; CON, cingulo-opercular network; DMN, default mode network; FPN, frontoparietal network; ON, occipital network; SMN, sensorimotor network. * $p < .05$. ** $p < .01$, *** $p < .005$.

Table 2. Nodes with the top 5% of node metrics of reappraisal and suppression

Reappraisal				Suppression			
RSNs	Brain regions	MNI coordinates (x,yz)	*Deg*	RSNs	Brain regions	MNI coordinates (x,yz)	*Deg*
SMN	Frontal Inf Oper L	-55 7 23	31.85 ± 47.91	SMN	Frontal Inf Oper L	-55 7 23	32.67 ± 48.65
FPN	Parietal Inf L	-41 -40 42	30.93 ± 50.43	FPN	Frontal Inf Tri L	-52 28 17	31.33 ± 48.4
FPN	Frontal Mid L	-42 7 36	30.52 ± 48.06	FPN	Parietal Inf L	-41 -40 42	31.26 ± 49.55
FPN	Parietal Inf L	-35 -46 48	30.33 ± 50.17	FPN	Frontal Mid L	-42 7 36	31.22 ± 47.45
SMN	Postcentral L	-41 -31 48	30.11 ± 49.55	SMN	Postcentral L	-41 -31 48	30.78 ± 48.27
CON	Temporal R	43 -43 8	29.78 ± 50.31	FPN	Parietal Inf L	-35 -46 48	30.67 ± 49.09
FPN	Frontal Inf Tri L	-52 28 17	29.56 ± 49.35	CON	Thalamus L	-12 -12 6	30.59 ± 48.01
SMN	SupraMarginal L	-54 -22 22	29.22 ± 47.98	CON	SupraMarginal L	-55 -44 30	30.56 ± 48.09

RSNs	Brain regions	MNI coordinates (x,yz)	*BC*	RSNs	Brain regions	MNI coordinates (x,yz)	*BC*
DMN	Frontal Inf Orb R	46 39 -15	1546.07 ± 4825.53	DMN	Frontal Inf Orb R	46 39 -15	1559 ± 4988.69
ON	Occipital Mid L	-29 -88 8	671.93 ± 2395.36	CN	Cerebellum Crus1 R	32 -61 -31	1109.74 ± 4337.28
DMN	Angular R	45 -72 29	470.7 ± 1577.85	FPN	Parietal Inf L	-35 -46 48	913.22 ± 4321.19
ON	Calcarine L	-4 -94 12	443.33 ± 2158.28	ON	Occipital Mid L	-29 -88 8	726.56 ± 2691.04
ON	Occipital Mid R	27 -91 2	421.52 ± 1261.23	ON	Calcarine L	-4 -94 12	674.41 ± 2555.33
SMN	Temporal R	46 -8 24	417.33 ± 1246.91	FPN	Parietal Inf L	-53 -50 39	491.19 ± 1685.59
CON	Temporal Inf R	54 -31 -18	376.78 ± 1273.32	DMN	Temporal Mid R	52 -15 -13	408.04 ± 1272.76
CON	Thalamus L	-12 -12 6	350.26 ± 1100.04	CON	Temporal Inf R	54 -31 -18	399.63 ± 1273.93

Table 2 Values indicate mean ± standard deviation. *Deg*, degree; *BC*, betweenness centrality; L, left; R, right; Sup, superior; Mid, middle; Inf, inferior; Med, medial; Ant, anterior; Post, posterior; Tri, triangularis; Oper, opercular; Supp, supplementary; RSN, resting-state network; CN, cerebellum network; CON, cingulo-opercular network; DMN, default mode network; FPN, frontoparietal network; ON, occipital network; SMN, sensorimotor network.

the betweenness centrality of every node was examined. While the left inferior parietal (MNI coordinates = -53, -50, 39) among the members of the FPN had the highest number of times to act as a bridge along the shortest path between two other nodes (*BC* = 312.67) in the whole-brain network of reappraisal, the left inferior parietal (MNI coordinates = -35, -46, 48) in the whole-brain network of suppression (*BC* = 913.22). Moreover, the right precentral gyrus (MNI coordinates = 46, -8, 24) among the members of the SMN found to play the most critical region in mediating the information transfer in the whole-brain network of reappraisal (*BC* = 417.33), while in the whole-brain network of suppression, the right precentral gyrus (MNI coordinates = 41, -23, 55) was found have the highest betweenness centrality (*BC* = 358.30).

On the other hand, in the case of CN, CON, DMN, and ON, the same area was found to be the most important in both reappraisal and suppression networks. Among the members of the CN, the right crus 1 cerebellum (MNI coordinates = 32, -61, -31) had the most control over the whole-brain reappraisal network (*BC* = 338.37) and the suppression network (*BC* = 1109.74). Among the areas belonging to the CON, the right inferior temporal gyrus (MNI coordinates = 54, -31, -18) had the most considerable influence over the whole-brain reappraisal network (*BC* = 376.78) and the suppression network (*BC* = 399.63). Likewise, the right inferior orbitofrontal gyrus (MNI coordinates = 46, 39, -15) of the DMN and the left middle occipital gyrus (MNI coordinates = -29, 88, 8) of the ON were found to commonly play a crucial role in transferring information in the whole-brain network of reappraisal and suppression.

3.2.3. Mean FC differences in intra- and inter-RSN connectivity

The difference of the strength of inter-RSN connectivity between reappraisal and suppression is displayed in Table 3. Results revealed that the intra-CN FC was significantly higher in suppression than reappraisal.

Table 3. Mean FC differences in inter-RSN connectivity

	CN	CON	DMN	FPN	ON	SMN
CN	.59 ± .78 (-2.44*) .66 ± .83	.27 ± .58 (.27)	.23 ± .50 (.63)	.22 ± .53 (.39)	.28 ± .61 (-1.15)	.25 ± .57 (.59)
CON	.26 ± .52	.42 ± .72 (.35) .41 ± .68	.29 ± .60 (.45)	.35 ± .70 (-.12)	.27 ± .66 (.84)	.38 ± .77 (.67)
DMN	.21 ± .41	.28 ± .55	.29 ± .51 (.47) .28 ± .45	.28 ± .60 (.17)	.25 ± .59 (.71)	.29 ± .63 (.12)
FPN	.20 ± .45	.35 ± .66	.28 ± .55	.43 ± .71 (.46) .42 ± .66	.27 ± .67 (.58)	.37 ± .75 (-.02)
ON	.30 ± .60	.26 ± .58	.23 ± .50	.25 ± .58	.43 ± .73 (.03) .43 ± .69	.28 ± .69 (.98)
SMN	.22 ± .47	.37 ± .71	.28 ± .58	.37 ± .69	.25 ± .59	.50 ± .78 (.67) .48 ± .72

Table 3 Paired t-tests were performed to examine the difference in mean FC between reappraisal and suppression. Values above the diagonal (lighter grey-colored cells) indicate mean ± standard deviation of reappraisal and t value in the parentheses; values under the diagonal (darker grey-colored cells) are mean ± standard deviation of suppression. On the diagonal, upper values are those of reappraisal, and lower values are those of suppression. CN, cerebellum network; CON, cingulo-opercular network; DMN, default mode network; FPN, frontoparietal network; ON, occipital network; SMN, sensorimotor network. * $p < .05$.

3.3. Dynamic network analysis

3.3.1. Network metrics of the whole-brain network and the six RSNs

In general, the statistical difference in the network metrics of the whole-brain network between reappraisal and suppression was prominent in the late runs (e.g., runs 3 and 4). As depicted in Table 4 and Fig. 3, except for the significantly higher modularity of reappraisal at the 26th window of run 2 than suppression, there was no difference in modularity between the conditions. On the other hand, the efficiency of information transfer across the network was higher in the late windows of run 3 and early windows of run 4 of suppression than reappraisal.

The statistical differences in the network metrics of the six RSNs between reappraisal and suppression are described in Table 5. Paired *t*-tests showed that, at a few windows, the CN, DMN, and FPN of suppression

Table 4. Significant differences in network metrics of the whole-brain network between reappraisal and suppression in dynamic analysis

	Q_{max}			E_{glob}		
Temporal Feature	Reapprais-al	Suppression	*t* value	Reapprais-al	Suppression	*t* value
R2W17	.53 ± .17	.58 ± .20	-1.30	.04 ± .07	.02 ± .04	2.14*
R2W26	.58 ± .20	.48 ± .23	2.63*	.05 ± .10	.03 ± .07	.67
R3W26	.52 ± .20	.55 ± .25	-.67	.02 ± .03	.06 ± .09	-2.24*
R3W27	.51 ± .23	.57 ± .22	-1.33	.01 ± .03	.06 ± .10	-2.33*
R4W3	.48 ± .18	.49 ± .19	.02	.03 ± .06	.07 ± .11	-2.52*
R4W5	.53 ± .19	.50 ± .27	.73	.02 ± .04	.05 ± .09	-2.19*

Table 4 Paired *t*-tests were performed to examine the difference in network metrics between reappraisal and suppression. Values indicate mean ± standard deviation. Q_{max}, modularity; E_{glob}, global efficiency; R, run; W, window.
* $p < .05$, ** $p < .01$.

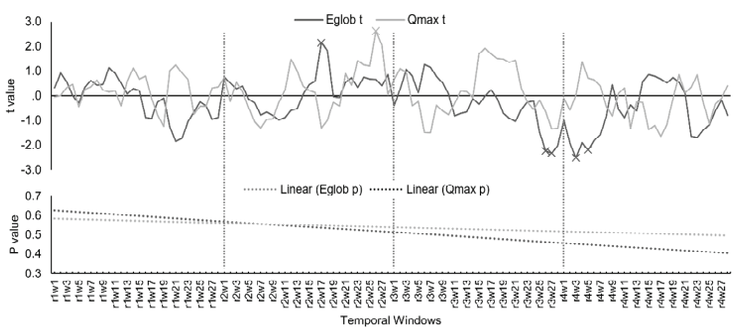

Fig. 3. Temporal change of the statistical difference of the network metrics between the whole-brain network of reappraisal and suppression. The linear trend lines of p values of modularity (Q_{max}) and global efficiency (E_{glob}) show that there was a minimal trend of the increasing statistically significant difference between reappraisal and suppression as window proceeds. Vertical dotted lines represent the boundary of the run. × denotes a statistically significant ($p < .05$) window

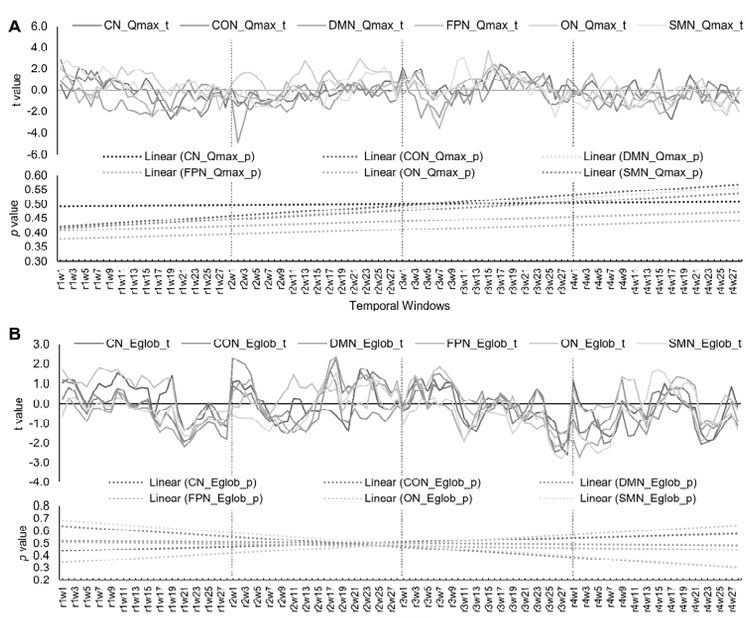

Fig. 4. Temporal change of the statistical difference of network metrics between the six RSNs of reappraisal and suppression. The temporal change of *t* value (upper panel) and the linear trend of *p*-value (lower panel) of the paired t-tests on modularity (A) and global efficiency (B) of the six RSNs between reappraisal and suppression are displayed. Vertical dotted lines represent the boundary of the run. Q_{max}, modularity; E_{glob}, global efficiency; CN, cerebellum network; CON, cingulo-opercular network; DMN, default mode network; FPN, frontoparietal network; ON, occipital network; SMN, sensorimotor network

Table 5. Significant differences in network metrics between the whole-brain network and the six RSNs of reappraisal and suppression in dynamic analysis

RSNs	Temp. Feature	Reappraisal	Suppression	t value	RSNs	Temp. Feature	Reappraisal	Suppression	t value
		Q_{max}					E_{glob}		
CN	R1W4	.35 ± .28	.2 ± .25	2.09*	CN	R3W27	.02 ± .09	.09 ± .19	-2.20*
	R1W19	.17 ± .23	.32 ± .29	-2.69*		R3W28	0 ± .06	.09 ± .18	-2.60*
	R1W20	.19 ± .23	.33 ± .27	-2.14*	CON	R2W18	.03 ± .09	-.01 ± .02	2.27*
	R3W1	.41 ± .28	.27 ± .27	2.07*		R3W26	-.01 ± .02	.04 ± .10	-2.48*
	R3W17	.47 ± .25	.3 ± .29	2.42*		R3W27	.04 ± .1	-.01 ± .01	-2.34*
	R3W18	.48 ± .26	.35 ± .26	2.09*		R4W22	0 ± .02	.04 ± .10	-2.07*
	R4W17	.21 ± .26	.39 ± .26	-2.79**	DMN	R1W21	0 ± .03	.05 ± .13	-2.19*
CON	R1W1	.31 ± .26	.12 ± .21	2.89**		R2W1	.05 ± .11	0 ± .02	2.30*
	R1W24	.14 ± .19	.29 ± .27	-2.50*		R2W2	.04 ± .1	0 ± .02	2.13*
	R3W16	.39 ± .30	.25 ± .29	2.10*	FPN	R1W21	-.01 ± .05	.08 ± .21	-2.16*
DMN	R1W14	.44 ± .14	.53 ± .14	-2.26*		R2W17	.02 ± .07	-.01 ± .02	2.14*
	R1W15	.43 ± .14	.51 ± .12	-2.14*		R2W18	.02 ± .06	-.01 ± .03	2.36*
	R1W16	.41 ± .17	.52 ± .11	-2.40*		R3W26	-.01 ± .03	.06 ± .16	-2.19*
	R2W2	.42 ± .13	.57 ± .14	-4.87**		R3W27	-.01 ± .03	.07 ± .18	-2.10*
	R2W3	.45 ± .17	.57 ± .14	-3.02**		R4W2	0 ± .04	.04 ± .09	-2.73*
	R2W10	.51 ± .12	.58 ± .14	-2.10*		R4W3	0 ± .06	.04 ± .12	-2.08*
	R3W4	.53 ± .15	.60 ± .17	-2.62*		R4W5	-.01 ± .03	.03 ± .1	-2.13*
	R3W7	.47 ± .15	.57 ± .16	-2.54*	SMN	R3W26	.01 ± .04	.07 ± .1	-2.59*
FPN	R1W16	.21 ± .26	.39 ± .21	-2.51*		R3W27	0 ± .03	.07 ± .12	-2.78*
	R1W20	.18 ± .25	.33 ± .24	-2.41*		R3W27	.01 ± .04	.08 ± .14	-2.44*
	R1W24	.16 ± .23	.31 ± .28	-2.22*		R4W4	.02 ± .08	.06 ± .12	-2.19*
	R3W6	.28 ± .27	.41 ± .28	-2.50*		R4W5	.01 ± .04	.05 ± .08	-2.54*
	R3W7	.24 ± .28	.44 ± .26	-3.58**		R4W6	0 ± .03	.04 ± .08	-2.35*
	R3W16	.43 ± .27	.27 ± .26	2.43*		R4W7	0 ± .02	.05 ± .11	-2.18*
	R4W15	.34 ± .27	.48 ± .25	-2.25*					
ON	R1W18	.51 ± .20	.37 ± .26	2.24*					
	R2W13	.54 ± .26	.36 ± .32	2.74*					
	R2W22	.61 ± .11	.47 ± .24	2.97**					
	R2W23	.58 ± .10	.46 ± .26	2.18*					
	R3W15	.53 ± .17	.38 ± .23	3.68**					
	R4W26	.37 ± .26	.53 ± .21	-2.39*					
SMN	R1W1	.39 ± .21	.24 ± .27	2.17*					
	R1W2	.43 ± .24	.25 ± .23	2.80**					
	R1W3	.38 ± .24	.25 ± .24	2.21*					
	R1W4	.39 ± .21	.26 ± .26	2.21*					
	R1W8	.41 ± .21	.25 ± .27	2.24*					
	R2W26	.45 ± .33	.29 ± .25	2.20*					
	R3W10	.50 ± .25	.31 ± .27	2.6**					
	R3W11	.51 ± .27	.33 ± .26	3.10**					
	R3W16	.48 ± .24	.36 ± .27	2.27*					
	R3W26	.34 ± .24	.45 ± .24	-2.53*					

Table 5 Paired t-tests were performed to examine the difference in network metrics between reappraisal and suppression. Values indicate mean ± standard deviation. Temp, Temporal; Q_{max}, modularity; E_{glob}, global efficiency; R, run; W, window; RSNs, resting-state networks; WBN, whole-brain network; CN, cerebellum network; CON, cingulo-opercular network; DMN, default mode network; FPN, frontoparietal network; ON, occipital network; SMN, sensorimotor network.
* $p < .05$. ** $p < .01$.

Table 6. Significant mean FC differences in intra- and inter RSN connectivity

RSN FC	Temporal Feature	Reappraisal	Suppression	*t* value
CN-CN	R3W28	.02 ± .04	.07 ± .11	-2.28*
CON-CON	R2W17	.01 ± .03	.01 ± .01	2.14*
	R2W18	.02 ± .03	.01 ± .01	2.22*
	R3W26	.01 ± .01	.03 ± .04	-2.60*
	R3W27	.01 ± .01	.03 ± .05	-2.20*
DMN-DMN	R2W1	.03 ± .05	.01 ± .01	2.28*
	R2W2	.03 ± .05	.01 ± .01	2.08*
FPN-FPN	R2W17	.02 ± .03	.01 ± .01	2.42*
	R2W18	.03 ± .04	.01 ± .01	2.53*
	R3W26	.01 ± .02	.05 ± .09	-2.13*
	R4W2	.02 ± .02	.03 ± .04	-2.28*
SMN-SMN	R3W26	.01 ± .02	.03 ± .04	-2.41*
	R3W27	.01 ± .01	.04 ± .05	-2.69*
	R3W28	.01 ± .02	.04 ± .06	-2.45*
	R4W4	.02 ± .03	.04 ± .05	-2.50*
	R4W5	.01 ± .02	.03 ± .04	-2.39*
	R4W6	.01 ± .01	.03 ± .04	-2.38*
	R4W7	.01 ± .01	.03 ± .05	-2.16*
CN-FPN	R1W1	.01 ± .02	.00 ± .02	2.17*
CN-SMN	R2W26	.00 ± .01	.00 ± .00	2.15*
	R4W15	.00 ± .01	.00 ± .00	2.06*
CON-FPN	R2W18	.03 ± .06	.01 ± .01	2.28*
	R3W26	.01 ± .01	.05 ± .09	-2.21*
CON-ON	R4W23	.00 ± .01	.02 ± .04	-2.06*
CON-SMN	R3W26	.01 ± .01	.02 ± .04	-2.37*
DMN-FPN	R2W17	.02 ± .03	.01 ± .01	2.27*
	R4W3	.01 ± .02	.03 ± .05	-2.06*
FPN-SMN	R4W4	.01 ± .02	.02 ± .05	-2.45*
	R4W5	.01 ± .01	.02 ± .03	-2.21*
	R4W6	.00 ± .01	.02 ± .04	-2.07*
ON-SMN	R3W25	.00 ± .01	.01 ± .01	-2.09*
	R3W26	.00 ± .00	.01 ± .02	-2.55*
	R4W3	.01 ± .01	.02 ± .03	-2.15*

Table 6 Paired *t*-tests were performed to examine the difference in the strength of intra-RSN connectivity between reappraisal and suppression. Values indicate mean ± standard deviation. RSN, resting-state network; FC, functional connections; R, run; W, window; CN, cerebellum network; CON, cingulo-opercular network; DMN, default mode network; FPN, frontoparietal network; ON, occipital network; SMN, sensorimotor network.
* $p < .05$

had significantly higher Q_{max} than reappraisal ($p < .01$). On the contrary, at a few windows, the CON, ON, and SMN of reappraisal had significantly higher Q_{max} than suppression. In addition, among the windows showing a significant difference in E_{glob} between reappraisal and suppression at a relatively lenient threshold, $p < .05$, windows of the CN, CON, FPN and SMN of suppression generally showed higher E_{glob} compared to reappraisal, and windows of the DMN of reappraisal showed higher E_{glob} compared to suppression. There was no significant difference between reappraisal and suppression in ON at any temporal level. Fig. 4A shows that all six RSNs

displayed a linear trend of decreasing statistical significance of the paired *t*-test on Q_{max} between reappraisal and suppression over time. On the other hand, while the CON, DMN, FPN, and SMN displayed a linear trend of increasing statistical significance of the paired t-test on E_{glob} between reappraisal and suppression over time, the CN and ON had a decreasing linear trend (Fig. 4B).

3.3.2. Mean FC differences in intra- and inter-RSN connectivity

Table 6 shows that, except for the ON, all RSNs had at least one temporal window showing a statistical difference in intra-network FC between reappraisal and suppression. The mean intra-CON FC of reappraisal was higher at run 2 and lower at run 3 than suppression. The mean intra-DMN of reappraisal was higher at run 2 than suppression. The mean intra-FPN FC of reappraisal was higher at run 2 and lower at run 3 and run 4 than suppression. The mean intra-SMN FC of reappraisal was lower at run 3 and run 4 than suppression. In most of the cases, significant differences in the strength of inter-RSN connectivity between reappraisal and suppression were found at the windows of run 4. The FC between the FPN and CN, CON, and DMN revealed significantly higher FC of reappraisal than suppression, while other significant FCs showed meaningfully higher FC of suppression than reappraisal.

4. Discussion

This is the first study that systematically examines the large-scale whole-brain functional network and the six sub-networks of reappraisal and suppression. It is also the first to investigate the temporal change of network metrics of the whole-brain network and six sub-networks and provide empirical neuroimaging evidence for the temporal features of the theoretical process model of emotion regulation (Gross, 2002; Gross & John, 2003).

4.1. Better regulatory performance of and the significance of the fronto-temporo-occipital regions for reappraisal

Although only a trend, the behavioral results reveal that reappraisal is a more effective strategy to regulate negative emotions than suppression; which is consistent with the overwhelming majority of studies (Hofmann, Heering, Sawyer, & Asnaani, 2009; Wang, Yang, & Wang, 2014). The findings provide indirect evidence that antecedent-focused strategies are more effective in the down-regulation of emotion than response-focused strategies. Although the left frontal regions and left inferior parietal regions were found to have the most functional connections with other brain regions (i.e., degree) in the whole-brain reappraisal network, the right inferior orbitofrontal gyrus, middle occipital regions, and temporal regions had the most controlling power over the fastest information transfer between the other two brain regions in the whole-brain network of reappraisal (Table 2).

4.2. The significance of the CN and FPN for suppression

Although the scientific discussions of the role of the CN had mainly been confined to its motor functions (Glickstein, 2007), there is an increasing recognition that the cerebellum contributes to emotion processing, emotion regulation (Schmahmann & Caplan, 2006; Schutter & van Honk, 2005; Turner et al., 2007), and that there is a functional relationship between the CN and multiple high-order networks including the FPN and DMN (Brissenden, Levin, Osher, Halko, & Somers, 2016; Buckner, Krienen, Castellanos, Diaz, & Yeo, 2011). Furthermore, the anatomical connections of the cerebellum with other brain regions involved in emotion regulation and in the perception of socially salient emotional material are also noteworthy (Schmahmann & Caplan, 2006). The cerebellum has connections with limbic

regions (e.g., the amygdala and the hippocampus) (Anand, Malhotra, Singh, & Dua, 1959) responsible for emotional response and memory, with brain stem areas containing neurotransmitters (e.g., serotonin, norepinephrine, and dopamine) involved in mood regulation (Dempesy et al., 1983; Marcinkiewicz, Morcos, & Chretien, 1989), and with the posterior parietal cortex and prefrontal regions (Dum & Strick, 2003; Kelly & Strick, 2003; Middleton & Strick, 2001). Other than its close relation to the CN as mentioned above, the FPN is involved in "phasic" aspects of attentional control (Sadaghiani et al., 2012), such as trial-by-trial adjustment of control (Seeley et al., 2007). In addition, the FPN is involved in modulating medial temporal lobules to suppress memory and negative emotions (Butler & James, 2010; Gagnepain, Hulbert, & Anderson, 2017).

In the present study, the CN and the FPN showed higher functional integration, or lower modularity, than reappraisal, and the intra-network connectivity of the CN was significantly higher than reappraisal (Table 1). Furthermore, the right crus 1 cerebellum of the CN and the left inferior parietal regions of the FPN were found to be responsible for the most important for passing the information (i.e., the high *BC*), leading to the higher controlling power over the whole-brain network (Table 2). Therefore, the CN and the FPN may contribute to the cognitive inhibition for suppression.

4.3. Reappraisal: early intra-DMN and late task-positive networks connectivity.

At the early windows of run 2, the DMN of reappraisal showed the higher efficiency of information transfer across the entire network than suppression (Table 5), and the intra-DMN connectivity of reappraisal was higher than suppression. In contrast, at the late windows of run 2, the intra-CON, intra-FPN, CN-FPN, CON-FPN, and DMN-FPN connectivity of reappraisal was higher than suppression (Table 6).

Revisiting the process theory of emotion regulation, the cognitive reappraisal should first notice the emotional stimuli, realize one's emotional response, and then engage several cognitive processes in interpreting the situation in a self-promoting way.

As previous studies have suggested that the DMN is associated with reflecting about one's own emotional state and understanding others' emotions (Andrews-Hanna, 2012; Andrews-Hanna, Smallwood, & Spreng, 2014), the robust activation of the DMN at the early stage of a run is consistent with the theory. Furthermore, the robust activation of task-positive networks, the CON and FPN, the strong functional connection with the CN which is known to contribute to the processing emotion and several other cognitive processes (Schmahmann & Caplan, 2006; Schutter & van Honk, 2005; Turner et al., 2007), and the DMN which is related to a wide range of spontaneous and self-generated processes, such as episodic future thinking and autobiographical memory processing (Andrews-Hanna et al., 2014; Pan et al., 2018) are all supporting the late-onset cognitive processes of reappraisal suggested by the process theory.

4.4. Suppression: early intra-DMN and late task-positive networks connectivity

At the early windows of run 4, the intra-SMN, DMN-FPN, FPN-SMN, and ON-SMN of suppression was higher than reappraisal. At the late windows within the late runs, the CN, CON, FPN, SMN, and the whole-brain network of suppression revealed the higher degree of information exchange across the whole network than reappraisal, and the intra-CN, intra-CON, intra-FPN, intra-SMN, CON-FPN, CON-ON, CON-SMN, and ON-SMN of suppression was higher than reappraisal (Tables 4-6).

At the early stage of suppression, the incoming visual stimuli and accompanying physiological responses, unbridled and not fully comprehended by further cognitive processes, may result in increased with the SMN. In addition, previous studies exhibited that

suppression leads one to judge one's own emotions, as well as others based on the visual stimulus via the PCC (Petrican, Rosenbaum, & Grady, 2015; Zaki, Hennigan, Weber, & Ochsner, 2010), which could explain the involvement of the DMN and the FPN for cognitive and self-referential processes. More importantly, consistent with the process model of emotion regulation, at the final stage, the task-positive networks (i.e., the CON and FPN) were extensively activated to regulate the behavioral affective responses and connected with the networks related to physiological responses (e.g., the SMN and ON) and emotional processing and responses (e.g., the CN).

The findings of the present study are the first empirical neuroimaging evidence that supports the theoretically suggested temporal difference between reappraisal and suppression (Gross & John, 1998, 2003; Lazarus & Alfert, 1964; Sheppes & Gross, 2011) by providing statistical differences of network metrics (i.e., the network efficiency and modularity) and the FC within- and between the RSNs between the reappraisal and suppression at both the large-scale level and the temporally segmented level, and identifying the hub brain regions for each strategy.

4.5. Limitation

As there are open questions about determining the proper window size for the SWC analysis, the fixed window size for this analysis was used to investigate the temporally varying functional network of each strategy. However, the use of a fixed window size may also have limited the scope of the study (Hutchison, Womelsdorf, Allen, et al., 2013). The window size governs the time-scale on which the analysis is performed; thus, it should be large enough to permit robust estimation of FC and accommodate the relatively slow frequencies of the BOLD signal, and yet small enough to detect potentially interesting transient changes in network connectivity. Previous studies have shown that window sizes of 30-60 s produce robust results in conventional acquisitions (Shirer et al., 2012). Topological descriptions of brain networks were found to stabilize at window lengths of approximately 30 s. The most appropriate frequencies and the best-fitting window size remain undetermined. Non-stationary and white noises in fMRI time series may remain even with the most robust preprocessing techniques. As these noises can form a particular pattern in common FC metrics and dynamic fluctuations of FC, cautious interpretation of the results is required.

In the present study, we adopted the experimental design that requires a long period of a run (about 13 minutes) and the unrandomized order of the blocks. Such design was intentionally devised to acquire an enough number of time points that allows the dynamic analysis and obtain stable and task-specific BOLD signals. In addition, the images used in the first and the second runs were reused in the third and the fourth runs because the number of negative images although the order of the images presented was randomized. Therefore, there is a potential risk that participants get adapted to the stimuli and such adaptation leads to better emotion regulation. In addition, the participants' residential environment, experience in negative events or seeing negative scenes, sensitiveness to certain type of negative images (e.g., insects, animals) were not considered in the present study. Future studies should be able to devise a way to separate the effect of adaptation to the stimuli and of the improved performance due to the repetition, and to consider various aspects of participants' background.

4.6. Need for the integration of static and dynamic functional connectivity

It has been very successful for the past few years to reveal certain characteristics of brain's functional coordination during both task and rest by averaging the functional connectivity and pursuing reproducibility and stability (Rogers, Morgan, Newton, & Gore, 2007;

Stoffers et al., 2015). However, the brain is a nonlinear complex system, and non-reproducibility of the brain is a necessary feature (Allen et al., 2014; Chang & Glover, 2010; Kiviniemi et al., 2011) that enables the generation of more features to characterize the uniqueness of each individual brain, making it possible to work as a potential biomarker(Jones et al., 2012; Sakoglu et al., 2010). Therefore, presenting the results of both dynamic and static aspects (Boissoneault, Letzen, Lai, Robinson, & Staud, 2018; Damaraju et al., 2014; Ramos-Nunez et al., 2017) in the data should be useful in that it allows us to understand and view the data property in a more integrated way.

5. Conclusions

This is the first study that provides neuroimaging evidence that supports the process model of emotion regulation by revealing the temporally varying network efficiency and intra- and inter-network functional connections of reappraisal and suppression. The present study provides novel insight into a potential neural mechanism for reappraisal and suppression using the network theory on the large-scale stationary functional connectivity analysis and the sliding window correlation analysis. Most interestingly, the present findings of temporally altering functional activity of the networks revealed that the DMN activates at the early stage of reappraisal and later the task-positive networks (e.g., the CON and FPN) and emotion-processing networks (e.g., the CN and DMN), and the SMN activates at the early stage of suppression and later the greater recruitment of task-positive networks and their functional connection with the emotional response-related networks (e.g., the SMN and ON). In addition, by examining a total of 160 brain regions, the present findings show the pivotal brain regions responsible for the global efficiency of the reappraisal and suppression networks.

Acknowledgements

For achieving true native expression and publishable quality, the manuscript has been edited for English language, grammar, punctuation, and spelling, as well as the formatting of the manuscript thoroughly, by Enago, the editing brand of Crimson Interactive Korea & Co.

REFERENCES

Allen, E. A., Damaraju, E., Plis, S. M., Erhardt, E. B., Eichele, T., & Calhoun, V. D. (2014). Tracking whole-brain connectivity dynamics in the resting state. *Cerebral Cortex*, *24*(3), 663-676. DOI: 10.1093/cercor/bhs352

Anand, B. K., Malhotra, C. L., Singh, B., & Dua, S. (1959). Cerebellar projections to limbic system. *Journal of Neurophysiology, 22*(4), 451-457. DOI: 10.1152/jn.1959.22.4.451

Andrews-Hanna, J. R. (2012). The brain's default network and its adaptive role in internal mentation. *Neuroscientist*, *18*(3), 251-270. DOI: 10.1177/1073858411403316

Andrews-Hanna, J. R., Smallwood, J., & Spreng, R. N. (2014). The default network and self-generated thought: component processes, dynamic control, and clinical relevance. *Annals of the New York Academy of Sciences*, *1316*, 29-52. DOI: 10.1111/nyas.12360

Bassett, D. S., Wymbs, N. F., Porter, M. A., Mucha, P. J., Carlson, J. M., & Grafton, S. T. (2011). Dynamic reconfiguration of human brain networks during learning. *Proceedings of the National Academy of Sciences of the United States of America*, *108*(18), 7641-7646. DOI: 10.1073/pnas.1018985108

Beck, A. T., & Steer, R. (1988). Beck anxiety inventory (BAI). BiB 2010, 54.

Boissoneault, J., Letzen, J., Lai, S., Robinson, M. E., & Staud, R. (2018). Static and dynamic functional connectivity in patients with chronic fatigue syndrome: use of arterial spin labelling fMRI.

Clinical Physiology and Functional Imaging, *38*(1), 128-137. DOI: 10.1111/cpf.12393

Braun, U., Schafer, A., Walter, H., Erk, S., Romanczuk-Seiferth, N., Haddad, L., ⋯ Bassett, D. S. (2015). Dynamic reconfiguration of frontal brain networks during executive cognition in humans. *Proceedings of the National Academy of Sciences of the United States of America*, *112*(37), 11678-11683. DOI: 10.1073/pnas.1422487112

Brissenden, J. A., Levin, E. J., Osher, D. E., Halko, M. A., & Somers, D. C. (2016). Functional Evidence for a Cerebellar Node of the Dorsal Attention Network. *Journal of Neuroscience*, *36*(22), 6083-6096. DOI: 10.1523/JNEUROSCI.0344-16.2016

Buckner, R. L., Krienen, F. M., Castellanos, A., Diaz, J. C., & Yeo, B. T. (2011). The organization of the human cerebellum estimated by intrinsic functional connectivity. *Journal of Neurophysiology*, *106*(5), 2322-2345. DOI: 10.1152/jn.00339.2011

Bullmore, E., & Sporns, O. (2009). Complex brain networks: graph theoretical analysis of structural and functional systems. *Nature Reviews Neuroscience*, *10*(3), 186-198. DOI: 10.1038/nrn2575

Butler, A. J., & James, K. H. (2010). The neural correlates of attempting to suppress negative versus neutral memories. *Cognitive, Affective, & Behavioral Neuroscience*, *10*(2), 182-194. DOI: 10.3758/CABN.10.2.182

Chang, C., & Glover, G. H. (2010). Time-frequency dynamics of resting-state brain connectivity measured with fMRI. *Neuroimage*, *50*(1), 81-98. DOI: 10.1016/j.neuroimage.2009.12.011

Cole, M. W., Reynolds, J. R., Power, J. D., Repovs, G., Anticevic, A., & Braver, T. S. (2013). Multi-task connectivity reveals flexible hubs for adaptive task control. *Nature Neuroscience*, *16*(9), 1348-1355. DOI: 10.1038/nn.3470

Cutuli, D. (2014). Cognitive reappraisal and expressive suppression strategies role in the emotion regulation: an overview on their modulatory effects and neural correlates. *Frontiers in Systems Neuroscience*, *8*, 175. DOI: 10.3389/fnsys.2014.00175

Damaraju, E., Allen, E. A., Belger, A., Ford, J. M., McEwen, S., Mathalon, D. H., ⋯ Calhoun, V. D. (2014). Dynamic functional connectivity analysis reveals transient states of dysconnectivity in schizophrenia. *NeuroImage: Clinical*, *5*, 298-308. DOI: 10.1016/j.nicl.2014.07.003

De Vico Fallani, F., Richiardi, J., Chavez, M., & Achard, S. (2014). Graph analysis of functional brain networks: practical issues in translational neuroscience. *Philosophical Transactions of the Royal Society B: Biological Sciences*, *369*(1653). DOI: 10.1098/rstb.2013.0521

Dempesy, C. W., Tootle, D. M., Fontana, C. J., Fitzjarrell, A. T., Garey, R. E., & Heath, R. G. (1983). Stimulation of the paleocerebellar cortex of the cat: increased rate of synthesis and release of catecholamines at limbic sites. *Biological Psychiatry*, *18*(1), 127-132.

Di, X., & Biswal, B. B. (2015). Dynamic brain functional connectivity modulated by resting-state networks. *Brain Structure and Function*, *220*(1), 37-46. DOI: 10.1007/s00429-013-0634-3

Di, X., Fu, Z., Chan, S. C., Hung, Y. S., Biswal, B. B., & Zhang, Z. (2015). Task-related functional connectivity dynamics in a block-designed visual experiment. *Frontiers in Human Neuroscience*, *9*, 543. DOI: 10.3389/fnhum.2015.00543

Dosenbach, N. U., Fair, D. A., Miezin, F. M., Cohen, A. L., Wenger, K. K., Dosenbach, R. A., . . . Petersen, S. E. (2007). Distinct brain networks for adaptive and stable task control in humans. *Proceedings of the National Academy of Sciences of the United States of America*, *104*(26), 11073-11078. DOI: 10.1073/pnas.0704320104

Dosenbach, N. U., Nardos, B., Cohen, A. L., Fair, D. A., Power, J. D., Church, J. A., ⋯ Schlaggar, B. L. (2010). Prediction of individual brain maturity using fMRI. *Science*, *329*(5997), 1358-1361. DOI: 10.1126/science.1194144

Dosenbach, N. U., Visscher, K. M., Palmer, E. D., Miezin, F. M., Wenger, K. K., Kang, H. C., . . . Petersen, S. E. (2006). A core system for the implementation of task sets. *Neuron*, *50*(5), 799-812. DOI: 10.1016/j.neuron.2006.04.031

Dum, R. P., & Strick, P. L. (2003). An unfolded map of the cerebellar dentate nucleus and its projections to the cerebral cortex. *Journal of Neurophysiology*, *89*(1), 634-639. DOI: 10.1152/jn.00626.2002

Fair, D. A., Cohen, A. L., Power, J. D., Dosenbach, N. U., Church, J. A., Miezin, F. M., . . . Petersen, S. E. (2009). Functional brain networks develop from a "local to distributed" organization. *PLoS Computational Biology*, *5*(5), e1000381. DOI: 10.1371/journal.pcbi.1000381

Fornito, A., Harrison, B. J., Zalesky, A., & Simons, J. S. (2012). Competitive and cooperative dynamics of large-scale brain functional networks supporting recollection. *Proceedings of the National Academy of Sciences of the United States of America*, *109*(31), 12788-12793. DOI: 10.1073/pnas.1204185109

Friston, K. J., Williams, S., Howard, R., Frackowiak, R. S., & Turner, R. (1996). Movement-related effects in fMRI time-series. *Magnetic Resonance in Medicine*, *35*(3), 346-355.

Gagnepain, P., Hulbert, J., & Anderson, M. C. (2017). Parallel Regulation of Memory and Emotion Supports the Suppression of Intrusive Memories. *Journal of Neuroscience*, *37*(27), 6423-6441. DOI: 10.1523/JNEUROSCI.2732-16.2017

Glickstein, M. (2007). What does the cerebellum really do? *Current Biology*, *17*(19), R824-827. DOI: 10.1016/j.cub.2007.08.009

Gross, J. J. (2002). Emotion regulation: affective, cognitive, and social consequences. *Psychophysiology*, *39*(3), 281-291. DOI: 10.1017.S0048577201393198

Gross, J. J., & John, O. P. (1998). Mapping the domain of expressivity: multimethod evidence for a hierarchical model. *Journal of Personality and Social Psychology*, *74*(1), 170-191.

Gross, J. J., & John, O. P. (2003). Individual differences in two emotion regulation processes: implications for affect, relationships, and well-being. *Journal of Personality and Social Psychology*, *85*(2), 348-362.

Hayes, J. P., Morey, R. A., Petty, C. M., Seth, S., Smoski, M. J., McCarthy, G., & Labar, K. S. (2010). Staying cool when things get hot: emotion regulation modulates neural mechanisms of memory encoding. *Frontiers in Human Neuroscience*, *4*, 230. DOI: 10.3389/fnhum.2010.00230

Hofmann, S. G., Heering, S., Sawyer, A. T., & Asnaani, A. (2009). How to handle anxiety: The effects of reappraisal, acceptance, and suppression strategies on anxious arousal. *Behaviour Research and Therapy*, *47*(5), 389-394. DOI: 10.1016/j.brat.2009.02.010

Hutchison, R. M., Womelsdorf, T., Allen, E. A., Bandettini, P. A., Calhoun, V. D., Corbetta, M., ⋯ Chang, C. (2013). Dynamic functional connectivity: promise, issues, and interpretations. *Neuroimage*, *80*, 360-378. DOI: 10.1016/j.neuroimage.2013.05.079

Hutchison, R. M., Womelsdorf, T., Gati, J. S., Everling, S., & Menon, R. S. (2013). Resting-state networks show dynamic functional connectivity in awake humans and anesthetized macaques. *Human Brain Mapping*, *34*(9), 2154-2177. DOI: 10.1002/hbm.22058

Jones, D. T., Vemuri, P., Murphy, M. C., Gunter, J. L., Senjem, M. L., Machulda, M. M., ⋯ Jack, C. R., Jr. (2012). Non-stationarity in the "resting brain's" modular architecture. *PLoS One*, *7*(6), e39731. DOI: 10.1371/journal.pone.0039731

Kelly, R. M., & Strick, P. L. (2003). Cerebellar loops with motor cortex and prefrontal cortex of a nonhuman primate. *Journal of Neuroscience*, *23*(23), 8432-8444.

Kiviniemi, V., Vire, T., Remes, J., Elseoud, A. A., Starck, T., Tervonen, O., & Nikkinen, J. (2011). A sliding time-window ICA reveals spatial variability of the default mode network in time. *Brain Connectivity*, *1*(4), 339-347. DOI: 10.1089/brain.2011.0036

Lazarus, R. S., & Alfert, E. (1964). Short-Circuiting of Threat by Experimentally Altering Cognitive Appraisal. *Journal of Abnormal Psychology*, *69*, 195-205.

Marcinkiewicz, M., Morcos, R., & Chretien, M. (1989). CNS connections with the median raphe nucleus: retrograde tracing with WGA-apoHRP-Gold complex in the rat. *Journal of Comparative Neurology*, *289*(1), 11-35. DOI: 10.1002/cne.902890103

Middleton, F. A., & Strick, P. L. (2001). Cerebellar projections to the prefrontal cortex of the primate.

Journal of Neuroscience, 21(2), 700-712.

Ochsner, K. N., & Gross, J. J. (2008). Cognitive Emotion Regulation: Insights from Social Cognitive and Affective Neuroscience. *Current Directions in Psychological Science*, *17*(2), 153-158. DOI: 10.1111/j.1467-8721.2008.00566.x

Ochsner, K. N., Ray, R. D., Cooper, J. C., Robertson, E. R., Chopra, S., Gabrieli, J. D., & Gross, J. J. (2004). For better or for worse: neural systems supporting the cognitive down- and up-regulation of negative emotion. *Neuroimage*, *23*(2), 483-499. DOI: 10.1016/j.neuroimage.2004.06.030

Pan, J., Zhan, L., Hu, C., Yang, J., Wang, C., Gu, L., ⋯ Wu, X. (2018). Emotion Regulation and Complex Brain Networks: Association Between Expressive Suppression and Efficiency in the Fronto-Parietal Network and Default-Mode Network. *Frontiers in Human Neuroscience*, *12*, 70. DOI: 10.3389/fnhum.2018.00070

Petrican, R., Rosenbaum, R. S., & Grady, C. (2015). Expressive suppression and neural responsiveness to nonverbal affective cues. Neuropsychologia, *77*, 321-330. DOI: 10.1016/j.neuropsychologia.2015.09.013

Ramos-Nunez, A. I., Fischer-Baum, S., Martin, R. C., Yue, Q., Ye, F., & Deem, M. W. (2017). Static and Dynamic Measures of Human Brain Connectivity Predict Complementary Aspects of Human Cognitive Performance. *Frontiers in Human Neuroscience*, *11*, 420. DOI: 10.3389/fnhum.2017.00420

Rogers, B. P., Morgan, V. L., Newton, A. T., & Gore, J. C. (2007). Assessing functional connectivity in the human brain by fMRI. *Magnetic Resonance Imaging*, *25*(10), 1347-1357. DOI: 10.1016/j.mri.2007.03.007

Rubinov, M., & Sporns, O. (2010). Complex network measures of brain connectivity: uses and interpretations. *Neuroimage*, *52*(3), 1059-1069. DOI: 10.1016/j.neuroimage.2009.10.003

Sadaghiani, S., Scheeringa, R., Lehongre, K., Morillon, B., Giraud, A. L., D'Esposito, M., & Kleinschmidt, A. (2012). alpha-band phase synchrony is related to activity in the fronto-parietal adaptive control network. *Journal of Neuroscience*, *32*(41), 14305-14310. DOI: 10.1523/JNEUROSCI.1358-12.2012

Sakoglu, U., Pearlson, G. D., Kiehl, K. A., Wang, Y. M., Michael, A. M., & Calhoun, V. D. (2010). A method for evaluating dynamic functional network connectivity and task-modulation: application to schizophrenia. *MAGMA*, *23*(5-6), 351-366. DOI: 10.1007/s10334-010-0197-8

Schmahmann, J. D., & Caplan, D. (2006). Cognition, emotion and the cerebellum. *Brain*, *129*(Pt 2), 290-292. DOI: 10.1093/brain/awh729

Schutter, D. J., & van Honk, J. (2005). The cerebellum on the rise in human emotion. *Cerebellum*, *4*(4), 290-294. DOI: 10.1080/14734220500348584

Seeley, W. W., Menon, V., Schatzberg, A. F., Keller, J., Glover, G. H., Kenna, H., ⋯ Greicius, M. D. (2007). Dissociable intrinsic connectivity networks for salience processing and executive control. *Journal of Neuroscience*, *27*(9), 2349-2356. DOI: 10.1523/JNEUROSCI.5587-06.2007

Sheppes, G., & Gross, J. J. (2011). Is timing everything? Temporal considerations in emotion regulation. *Personality and Social Psychology Review*, *15*(4), 319-331. DOI: 10.1177/1088868310395778

Shirer, W. R., Ryali, S., Rykhlevskaia, E., Menon, V., & Greicius, M. D. (2012). Decoding subject-driven cognitive states with whole-brain connectivity patterns. *Cerebral Cortex*, *22*(1), 158-165. DOI: 10.1093/cercor/bhr099

Stoffers, D., Diaz, B. A., Chen, G., den Braber, A., van't Ent, D., Boomsma, D. I., ⋯ Linkenkaer-Hansen, K. (2015). Resting-State fMRI Functional Connectivity Is Associated with Sleepiness, Imagery, and Discontinuity of Mind. *PLoS One*, *10*(11), e0142014. DOI: 10.1371/journal.pone.0142014

Takeuchi, H., Taki, Y., Nouchi, R., Yokoyama, R., Kotozaki, Y., Nakagawa, S., ⋯ Kawashima, R. (2017). Regional homogeneity, resting-state functional connectivity and amplitude of low frequency fluctuation associated with creativity measured by divergent thinking in a sex-specific manner. *Neuroimage*, *152*, 258-269. DOI: 10.1016/j.neuroimage.2017.02.079

Turner, B. M., Paradiso, S., Marvel, C. L., Pierson, R.,

Boles Ponto, L. L., Hichwa, R. D., & Robinson, R. G. (2007). The cerebellum and emotional experience. *Neuropsychologia*, *45*(6), 1331-1341. DOI: 10.1016/j.neuropsychologia.2006.09.023

van den Heuvel, M. P., & Hulshoff Pol, H. E. (2010). Exploring the brain network: a review on resting-state fMRI functional connectivity. *European Neuropsychopharmacology*, *20*(8), 519-534. DOI: 10.1016/j.euroneuro.2010.03.008

Wang, Y., Yang, L., & Wang, Y. (2014). Suppression (but not reappraisal) impairs subsequent error detection: an ERP study of emotion regulation's resource-depleting effect. *PLoS One*, *9*(4), e96339. DOI: 10.1371/journal.pone.0096339

Yan, C. G., Cheung, B., Kelly, C., Colcombe, S., Craddock, R. C., Di Martino, A., ⋯ Milham, M. P. (2013). A comprehensive assessment of regional variation in the impact of head micromovements on functional connectomics. *Neuroimage*, *76*, 183-201. DOI: 10.1016/j.neuroimage.2013.03.004

Zaki, J., Hennigan, K., Weber, J., & Ochsner, K. N. (2010). Social cognitive conflict resolution: contributions of domain-general and domain-specific neural systems. *Journal of Neuroscience*, *30*(25), 8481-8488. DOI: 10.1523/JNEUROSCI.0382-10.2010

원고접수: 2018.06.18
수정접수: 2018.09.17
게재확정: 2018.09.19